Influence of doping on the electronic transport in GaSb/InAs(Sb) nanowire tunnel devices

Borg, Mattias; Ek, Martin; Ganjipour, Bahram; Dey, Anil; Dick Thelander, Kimberly; Wernersson, Lars-Erik; Thelander, Claes

Published in:
Applied Physics Letters

DOI:
10.1063/1.4739082

2012

Influence of doping on the electronic transport in GaSb/InAs(Sb) nanowire tunnel devices

B. Mattias Borg, Martin Ek, Bahram Ganjipour, Anil W. Dey, Kimberly A. Dick et al.

Citation: Appl. Phys. Lett. **101**, 043508 (2012); doi: 10.1063/1.4739082
View online: http://dx.doi.org/10.1063/1.4739082
View Table of Contents: http://apl.aip.org/resource/1/APPLAB/v101/i4
Published by the American Institute of Physics.

Influence of doping on the electronic transport in GaSb/InAs(Sb) nanowire tunnel devices

B. Mattias Borg,[1,a)] Martin Ek,[2] Bahram Ganjipour,[1] Anil W. Dey,[3] Kimberly A. Dick,[1,2] Lars-Erik Wernersson,[3] and Claes Thelander[1,b)]
[1]*Solid State Physics, Lund University, Box 118, S-221 00 Lund, Sweden*
[2]*Polymer & Materials Chemistry, Lund University, Box 124, S-221 00 Lund, Sweden*
[3]*Department of Electrical- and Information Technology, Lund University, Box 118, S-221 00 Lund, Sweden*

(Received 7 May 2012; accepted 10 July 2012; published online 27 July 2012)

The effect of various doping profiles on the electronic transport in GaSb/InAs(Sb) nanowire tunnel diodes is investigated. Zn-doping of the GaSb segment increases both the peak current density and the current level in reverse bias. Top-gated diodes exhibit peak current modulation with a threshold voltage which can be controlled by Zn-doping the InAs(Sb) segment. By intentionally n-doping the InAs(Sb) segment degenerate doping on both sides of the heterojunction can be achieved, as well as tunnel diodes with peak current of 420 kA/cm^2 at $V_{DS} = 0.16$ V and a record-high current density of 3.6 MA/cm^2 at $V_{DS} = -0.5$ V. © *2012 American Institute of Physics*. [http://dx.doi.org/10.1063/1.4739082]

The GaSb/InAs heterostructure has an uncommon broken type II band alignment, for which the bottom of the conduction band in InAs lies below the top of the GaSb valence band. This broken gap leads to very efficient band-to-band tunneling, with the possibility of high current densities. With the recent focus on developing low-power devices, and in particular tunnel-field-effect transistors (TFETs), there is a renewed interest in staggered and broken-gap heterojunctions as they may enable high on-currents and steep subthreshold swing.[1–4] For transistor applications, it is also important to efficiently control the electric potential of the channel region, and the gate-all-around geometry made possible by the small diameter of nanowires enables gate modulation near the quantum capacitance limit.[5] It is thus highly relevant to realize broken-gap tunnel devices in nanowires. Recently, we demonstrated GaSb/InAs(Sb) nanowire Esaki diodes with high peak current levels and peak-to-valley current ratio (PVCR).[6] By optimizing the doping profiles of these heterostructures, it is hoped that even better performance can be achieved. Doping control may also be crucial for TFET applications, to enable potential modulation in selected parts of the device, as well as to control the threshold voltage and minimize access resistance. In this letter, we thus investigate the influence of p-doping (Zn) and n-doping (Se) on the performance of GaSb/InAs(Sb) nanowire tunnel diodes and present significantly improved device performance over earlier work. In addition, we explore the effects of various doping profiles on the temperature dependent *I–V* and the threshold voltage of top gated devices.

GaSb/InAs nanowires are grown from Au seed particles deposited on GaAs(111)B substrates in a manner similar to that which has been reported previously.[7] The GaSb/InAs heterojunction is characterized as being almost atomically abrupt, but with an Sb transient ($InAs_{1-x}Sb_x$) reaching into the InAs segment and decaying exponentially from $x = 0.3$–0.4 down to 0.03–0.07 over 5–13 nm. This segment will thus be denoted InAs(Sb) in the following. After growth, the samples are annealed in H_2 at 490 °C for 10 min to form a narrow constriction (neck) at the heterojunction.[8] This removes the short-circuit between the InAs(Sb) segment and an unintentionally formed InAs(Sb) shell (~3–5 nm thick) surrounding the GaSb nanowire. Doping of the nanowire heterostructures is performed *in-situ* by adding controlled amounts of diethylzinc (DEZn) or ditertiarybutylselenium (DTBSe) during the growth. Three different doping profiles were investigated: (A) Zn-doped GaSb and unintentionally doped InAs(Sb), (B) Zn-doped GaSb and Zn-doped InAs(Sb), and (C) Zn-doped GaSb and Se-doped InAs(Sb). For type A, several different Zn doping levels were investigated. The ratios between the doping precursor and group-III precursor flows are labelled Zn/Ga, Zn/In, or Se/In in the text and used as qualitative measure of the doping level.

The crystal structure of nanowires from all three types of samples was characterized using transmission electron microscopy. In all cases, the GaSb segment and the first 200–500 nm of the InAs(Sb) segment were pure zincblende, with the remainder containing a few (C) or many (A and B) twins but no wurtzite. Previous studies on InAs nanowires show that the electrical properties are not strongly affected unless inclusions of wurtzite are present.[9]

Single nanowire tunnel diodes were processed by breaking off nanowires and depositing them onto a patterned Si/SiO_2 chip. Electron beam lithography (EBL) was then used to define drain and source contacts to the GaSb and InAs(Sb) segments, respectively [Figs. 1(b) and 1(c)]. After EBL, the exposed areas were ashed in oxygen plasma, wet-etched for 5 s in 1:10 buffered HF, followed by evaporation/lift-off of 25 nm Ni and 75 nm Au. In order to investigate details in the charge transport, top gate electrodes were also fabricated to selected nanowires to cover the whole distance between the source and drain electrodes. The gate dielectric was processed using a second EBL step, atomic layer deposition of HfO_2 at 100 °C, and lift-off. Finally, the gate electrode was defined in a third EBL step, followed by Ni/Au metallization and lift-off.

a)Present address: IBM Research Zurich, Säumerstrasse 4, 8803 Rüschlikon, Switzerland.
b)Author to whom correspondence should be addressed. Electronic mail: claes.thelander@ftf.lth.se.

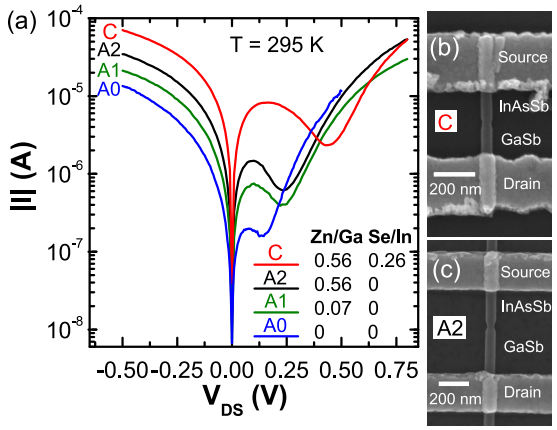

FIG. 1. (a) $|I|$-V characteristics of GaSb/InAs(Sb) tunnel diodes of type A and C. SEM images of (b) type C and (c) type A2 nanowire devices.

The electrical properties of the GaSb/InAs(Sb) nanowires were first characterized using two-terminal device geometries, with bias applied to the drain electrode and the source electrode kept grounded. The $|I|$-V characteristics of devices of type A and C are presented in Fig. 1(a). The A0, A1, and A2 devices have an increasing amount of Zn doping in the GaSb segments. In the type C sample, Se-doping has also been introduced during the growth of the InAs(Sb) segment. From this graph, it is clear that an increased Zn/Ga ratio during growth has a strong effect on the peak and reverse bias current levels of the GaSb/InAs(Sb) tunnel diodes, and that Se (n-) doping of the source provides a further, substantial improvement.

Sample A0, which is only unintentionally doped (Zn/Ga = 0), has a peak current of 191 nA and a PVCR of 1.3.[8] Sample A1 which was grown with Zn/Ga = 0.07 exhibits a much higher peak current level of 840 nA ($V_{DS} = 0.11$ V) and a PVCR of 2.1.[6] By further increasing the Zn doping in device A2 to Zn/Ga = 0.56, the peak current increases to 1.5 μA ($V_{DS} = 0.10$ V) with a PVCR of 2.4. These devices all have similar diameters in the neck-region (45 ± 5 nm), such that a direct comparison of current levels is possible. The improvement in peak current level between type A2 and A0 is thus almost an order of magnitude. On average, the peak voltage also shifts to slightly higher voltages for samples where Zn doping was used, consistent with a movement of the Fermi level in the GaSb nanowire towards the valence band edge. In reverse bias, the current level also increases with increased doping levels. Simulations of ideal GaSb/InAsSb tunnel diodes indicate that the reverse bias current should only be marginally affected by the p-side doping level.[6] The improved current observed here is instead attributed to a reduced series resistance in the GaSb segment. By normalizing to the neck cross-sectional area (Ø = 40 nm), a current density of 2.5 MA/cm^2 is obtained at $V_{DS} = -0.5$ V for the type A2 devices.

The type C device shown in Fig. 1(a), with Se (n-) doping in the InAs(Sb) segment, exhibits a peak current of 8.3 μA, which is much higher than the best type A device. The peak voltage is also considerably higher, 0.16 V, consistent with a higher Fermi level position in the InAs source. With a measured diameter in the neck region of 50 nm [Fig. 1(b)], the peak current density is 420 kA/cm^2, which gives the same scaled peak resistance as the tunnel diodes of Mohata *et al.*[10] with the highest peak current density reported to date (1 MA/cm^2 at 0.4 V). The PVCR is 3.6 at room-temperature for the type C device, indicating a very high-quality tunnel junction despite high doping levels. The current level in reverse bias is further improved (70 μA, 3.6 MA/cm^2 at $V_{DS} = -0.5$ V) compared to the type A devices, which we attribute to a strongly reduced series resistance, as is detailed later. The value for reverse-bias current density is almost a factor of two higher than the value reported by Mohata *et al.*[10]

Devices were also processed to include a top gate electrode covering the entire source-drain contact separation. A typical three terminal type A2 device is shown in Figs. 2(a) and 2(b) before and after processing. In agreement with Fig. 1(a), we find that such a device exhibits normally on device characteristics, and that application of a negative gate voltage reduces the peak current level [Fig. 2(c)]. For $V_{GD} = -2.0$ V, band-to-band tunneling is suppressed, such

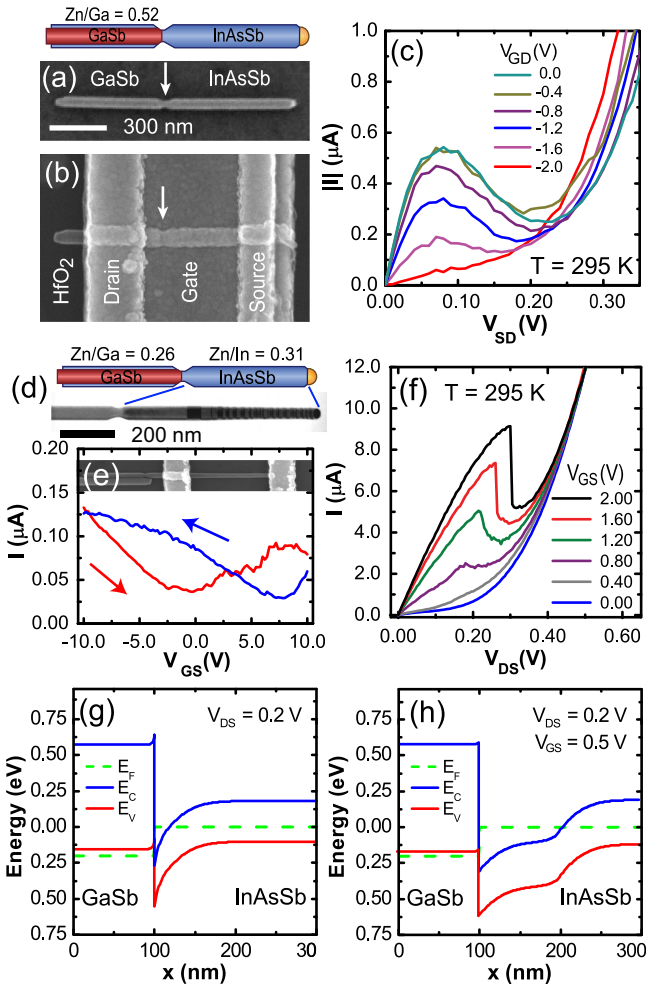

FIG. 2. Schematic and SEM images of a three terminal type A2 device (a) before and (b) after processing. (c) I-V characteristics of the same device for various applied gate voltages showing negative threshold voltage. (d) Schematic and bright-field TEM image of a type B nanowire. (e) Ambipolar I-V_{GS} characteristics in back-gated InAs(Sb) segments of type B nanowires, $V_{DS} = 100$ mV. The red and blue curves represent measurement data obtained for forward and reverse back-gate sweeps respectively. (f) I-V characteristics of a type B gated diode for various applied gate voltages showing positive threshold voltage. Calculated band diagrams of a type B device at $V_{DS} = 0.2$ V and (g) $V_{GS} = 0$ and (h) $V_{GS} = 0.5$ V.

that only the diode current of the *p-n* junction can be observed. We believe that the high Zn doping in the GaSb segment causes the applied gate potential to mostly affect the InAs(Sb) side of the heterojunction, thus allowing the gate to effectively shift the InAs(Sb) bands relative to the GaSb side. This is important since it relaxes the requirement for perfect gate alignment in the processing of early-stage TFET devices based on such structures.

In these devices, a negative V_{GD} is required to reach the off-state, but for TFET applications, a positive threshold voltage may be preferable. Thus, we also investigate type B devices with maintained Zn-doping throughout the entire GaSb/InAs(Sb) heterostructure. The conductivity of Zn-doped InAs(Sb) segments was evaluated by two terminal measurements. By using the Si substrate as a gate electrode, it was found that the nanowires exhibit ambipolar conduction [Fig. 2(e)], similar to what is elsewhere reported for Zn-doped InAs nanowires.[11,12] Typically, this ambipolarity is explained by an n-type surface channel in otherwise p-type InAs, because of surface Fermi level pinning within the conduction band of InAs. Ford *et al.* report that doping levels higher than 1×10^{19} cm^{-3} are needed to make InAs nanowires completely p-type.[12]

In contrast to the type A2 devices, top-gated type B tunnel diodes did not exhibit a clear peak in the current when forward biased at $V_{GS} = 0$ V. As a positive gate bias is applied, however, a peak develops, which shifts towards higher V_{DS} with increased applied V_{GS} [Fig. 2(f)]. For $V_{GS} = 2.0$ V, the peak current is as high as 9.1 μA at $V_{DS} = 0.3$ V (PVCR = 1.8), corresponding to a peak current density of 460 kA/cm^2 (Ø = 50 nm). This behavior can be explained by the p-doping of the InAs(Sb) segment, which gives an initial Fermi level position within the InAs(Sb) band gap. The strong upwards band bending on the InAs(Sb) side of the heterojunction thus blocks the BTBT current in forward bias [Fig. 2(g)]. With positive gate bias, the InAs(Sb) bands are pushed down and the BTBT current path into the GaSb valence band opens up [Fig. 2(h)]. For a large enough V_{DS}, however, the band bending will again be strong enough to close the channel, giving a region of negative differential conductance. In contrast to the type A2 devices, type B devices have a positive threshold voltage in forward bias. However, a reduced but significant tunnel current was observed in reverse bias even for $V_{GS} = 0$ V.

Three-terminal devices were also made of type C nanowires which have a Zn-doped GaSb segment (Zn/Ga = 0.56) and Se-doped InAs(Sb) segment (Se/In = 0.26) [Figs. 3(a) and 3(b)]. These devices show only a negligible gate response within a range of $V_{GS} = -1$ to 1 V, indicating that both segments are degenerately doped. Fig. 3(c) presents the temperature dependent *I-V* characteristics of the type C device depicted in Fig. 3(b). The very weak temperature dependence of the *I-V* in reverse bias and low forward bias (<0.3 V) demonstrates that the current transport is governed by BTBT at the GaSb-InAs(Sb) heterointerface. On a linear scale [Fig. 3(d)], one can distinguish that the current in the peak is actually increasing somewhat with reduced temperature. As only carriers with energies lower than that of the broken gap can contribute to direct band-to-band tunneling, we attribute the increased peak current to the reduced spreading of the Fermi distribution at lower temperature. This allows for more states to participate in the tunneling process[13] despite a slightly decreased broken gap size.[14]

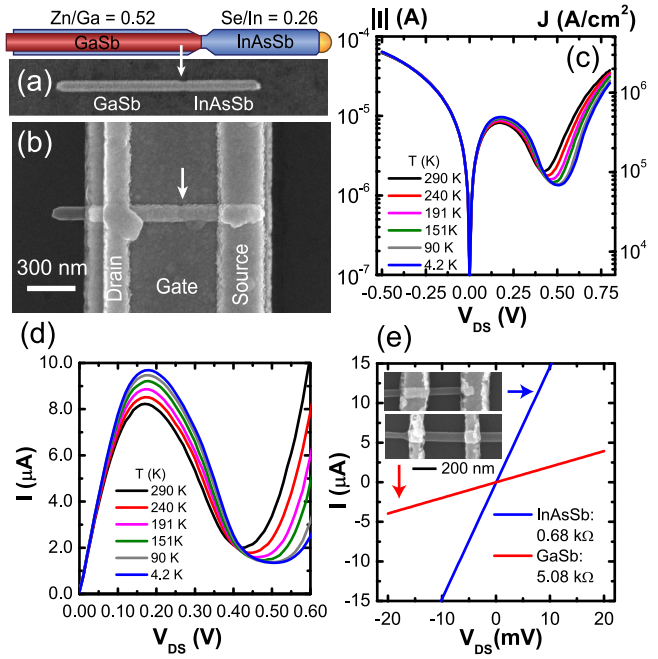

FIG. 3. Schematic and SEM images of a type C nanowire (a) before and (b) after processing into a three terminal device. Temperature dependent $|I|$-V characteristics of the same device in (c) logarithmic and (d) linear scale. (e) Resistance measurements of InAs(Sb) and GaSb segments on type C devices.

For larger forward bias (>0.3 V), the temperature dependence is stronger [Fig. 3(c)] since the current is dominated by emission of holes from the GaSb side to the InAs(Sb) side across the Schottky-like hole barrier formed at the heterojunction.[6] Bias dependent activation energies for this current were extracted from Arrhenius plots for both type A and C devices and are shown in Fig. 4(a). All types of devices exhibit similar nonlinearly increasing activation energy for decreasing bias, which drops again as the current becomes dominated by the tunnel current at low bias. At $V_{DS} = 0$ V, the activation energy should be equal to the built-in voltage of the p-n junction and similar in size to the valence band offset between GaSb and $InAs_{0.9}Sb_{0.1}$ (0.3–0.4 eV). Unfortunately, the non-linear curve shape precludes accurate extrapolation of the curves down to $V_{DS} = 0$ V.

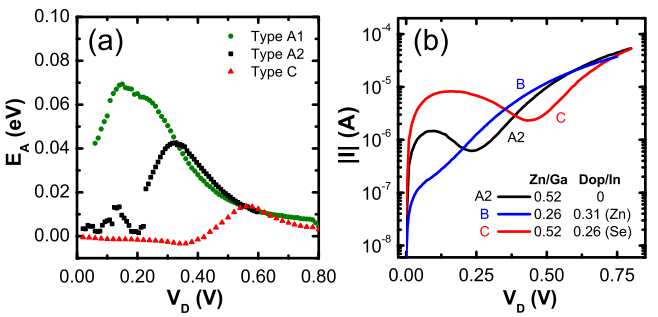

FIG. 4. (a) Extracted activation energies as a function of V_{DS} for type A1, A2, and C devices. (b) Comparison of *I-V* characteristics in forward bias for type A2, B, and C devices, where the effect of InAs(Sb) doping on the magnitude of the diode current is evident.

TABLE I. Summary of tunnel diode figures of merits and resistivity in type A-C GaSb/InAs(Sb) tunnel diodes.

Device type	Zn/Ga	*Dop/In*	I_{DS} at −0.5 V (MA/cm^2)	I_{peak} (kA/cm^2)	ρ_{GaSb}[a] (mΩ cm)	ρ_{InAsSb} (mΩ cm)
A0	0	0	0.55	8	40	3.4
A1	0.07	0	1.75	67	25	…
A2	0.52	0	2.2	94	7.1	…
B	0.26	0.31 (Zn)	0.16[b]	No peak[b]	…	80
C	0.52	0.26 (Se)	3.6	420	7.3	0.67

[a]ρ is here for the GaSb/InAs core/shell structure with ambipolar/semimetal character.
[b]Values are for $V_{GS} = 0$ V.

Another way to evaluate the built-in voltage is to compare the diode current levels. As is evident in Fig. 4(b), where the *I-V* of type A2, B, and C devices are compared, the diode current at a given V_{DS} is higher in type A devices compared to type C devices. This can be explained by the higher electron concentration in type C devices, which shifts the InAs(Sb) bands downwards leading to a larger built-in voltage. Apart from increasing the peak current level, n-side doping thus has the beneficial effect of decreasing the diode current, resulting in improved PVCR values. The opposite effect is evident in type B devices, which have the Fermi level within the InAs(Sb) band gap, and exhibit a higher diode current than both type A and C devices.

Finally, the resistivity of various GaSb and InAs(Sb) segments was evaluated by two-contact measurements on devices fabricated without a top-gate (Table I). For type C devices, the GaSb and InAs(Sb) segments exhibit linear *I–V* [Fig. 3(e)] with 2-terminal resistivity of 7.3 ± 1.8 mΩ cm and 0.67 ± 0.05 mΩ cm, respectively, averaged over three devices of each type. Both contacts are ohmic as seen from the temperature dependence of corresponding diodes in Figs. 2(c) and 2(d), where the device resistance decreases with reduced temperature. We find the resistivity for the Se-doped InAs(Sb) segments to be around 5 times lower than for the nominally undoped InAs(Sb) segments in type A0 devices. For the GaSb segments, we also find a factor of around 5 lower resistivity values in the case of type A2 and type C devices compared to type A0 devices. The key to reaching even higher current densities is to further reduce the GaSb series resistance, which is still an order of magnitude higher than that of the InAs(Sb) for type C devices. We estimate that roughly 50% of the diode resistance for the type C device presented in Fig. 1(b) is from series resistance in the GaSb. By reducing such parasitics, through further increasing the Zn doping level or minimizing the device length, we expect it should be possible to reach reverse current densities up to 6–7 MA/cm^2 in these structures at $V_{DS} = -0.5$ V.

In summary, we have investigated the effects of various doping profiles on the electronic transport in GaSb/InAs(Sb) nanowire tunnel diodes, as summarized in Table I. Increasing Zn-doping of the GaSb segment increases the peak current density as well as the current level in reverse bias. Top-gated devices show peak current modulation with a negative threshold voltage. By Zn-doping the InAs(Sb) segment, the threshold voltage can be shifted to positive voltages resulting in enhancement-mode operation. By introducing Se into the InAs(Sb) segment, degenerate doping on both sides of the heterojunction was achieved. For such structures we observed tunnel diode peak current densities up to 420 kA/cm^2 at 0.16 V and a record-high value of 3.6 MA/cm^2 at $V_{DS} = -0.5$ V.

This work was carried out with financial support from the Nanometer Structure Consortium at Lund University (nmC@LU), the Swedish Research Council (VR), the Swedish Foundation for Strategic Research (SSF), and the Knut and Alice Wallenberg Foundation (KAW).

[1]S. O. Koswatta, S. J. Koester, and W. Haensch, IEEE Trans. Electron Devices **57**, 3222 (2010).
[2]J. Knoch, in *International Symposium on VLSI Technology, Systems, and Applications, 2009, VLSI-TSA '09* (2009), pp. 45–46.
[3]R. Li, Y. Lu, G. Zhou, Q. Liu, S. D. Chae, T. Vasen, W. S. Hwang, Q. Zhang, P. Fay, T. Kosel, M. Wistey, H. Xing, and A. Seabaugh, IEEE Electron Dev. Lett. **33**, 363 (2012).
[4]M. T. Björk, H. Schmid, C. D. Bessire, K. E. Moselund, H. Ghoneim, S. Karg, E. Lörtscher, and H. Riel, Appl. Phys. Lett. **97**, 163501 (2010).
[5]K. Storm, G. Nylund, M. Borgström, J. Wallentin, C. Fasth, C. Thelander, and L. Samuelson, Nano Lett. **11**, 1127 (2011).
[6]B. Ganjipour, A. W. Dey, B. M. Borg, M. Ek, M.-E. Pistol, K. A. Dick, L.-E. Wernersson, and C. Thelander, Nano Lett. **11**, 4222 (2011)
[7]M. Ek, B. M. Borg, A. W. Dey, B. Ganjipour, C. Thelander, L.-E. Wernersson, and K. A. Dick, Cryst. Growth Des. **11**, 4588 (2011).
[8]B. M. Borg, M. Ek, K. A. Dick, B. Ganjipour, A. W. Dey, C. Thelander, and L.-E. Wernersson, Appl. Phys. Lett. **99**, 203101 (2011).
[9]C. Thelander, P. Caroff, S. Plissard, A. W. Dey, and K. A. Dick, Nano Lett. **11**, 2424 (2011).
[10]D. K. Mohata, D. Pawlik, L. Liu, S. Mookerjea, V. Saripalli, S. Rommel, and S. Datta, in *Device Research Conference*, June 21–23 (IEEE, South Bend, Indiana, 2010), pp. 103–104.
[11]B. S. Sørensen, M. Aagesen, C. B. Sørensen, P. E. Lindelof, K. L. Martinez, and J. Nygård, Appl. Phys. Lett. **92**, 012119 (2008)
[12]A. C. Ford, S. Chuang, J. C. Ho, Y.-L. Chueh, Z. Fan, and A. Javey, Nano Lett. **10**, 509 (2010).
[13]J. R. Söderström, D. H. Chow, and T. C. McGill, Appl. Phys. Lett. **55**, 1094 (1989).
[14]D. M. Symons, M. Lakrimi, M. van der Burgt, T. A. Vaughan, R. J. Nicholas, N. J. Mason, and P. J. Walker, Phys. Rev. B **51**, 1729–1734 (1995).